Multi-box mass balance model of PFOA and PFOS in different regions of San Francisco Bay

Francisco Sánchez-Soberón[1,2,*], Rebecca Sutton[3], Margaret Sedlak[3], Donald Yee[3], Marta Schuhmacher[1], June-Soo Park[4]

[1]Departament d'Enginyeria Quimica, Universitat Rovira i Virgili, Av. Països Catalans 26, 43007 Tarragona, Spain

[2]LEPABE — Laboratory for Process Engineering, Environment, Biotechnology and Energy, Faculty of Engineering, University of Porto, Rua Dr. Roberto Frias, 4200-465 Porto, Portugal

[3]San Francisco Estuary Institute, 4911 Central Ave, Richmond, CA 98404, United States

[4]Department of Toxic Substances Control, California Environmental Protection Agency, 700 Heinz Avenue, Berkeley, CA 94710, United States

*corresponfing author email: fssoberon@fe.up.pt; telephone: +351 22 041 4854

Abstract

We present a model to predict the long-term distribution and concentrations of perfluorooctanoic acid (PFOA) and perfluorooctanesulfonic acid (PFOS) in estuaries comprising multiple intercommunicated sub-embayments. To that end, a mass balance model including rate constants and time-varying water inputs was designed to calculate levels of these compounds in water and sediment for every sub-embayment. Subsequently, outflows and tidal water exchanges were used to interconnect the different regions of the estuary. To calculate plausible risks to population, outputs of the model were used as inputs in a previously designed model to simulate concentrations of PFOA and PFOS in a sport fish species (*Cymatogaster aggregata*). The performance of the model was evaluated by applying it to the specific case of San Francisco Bay, (California, USA), using 2009 sediment and water sampled concentrations of PFOA and PFOS in North, Central and South regions. Concentrations of these compounds in the Bay displayed

exponential decreasing trends, but with different shapes depending on region, compound, and compartment assessed. Nearly stable PFOA concentrations were reached after 50 years, while PFOS needed close to 500 years to stabilize in sediment and fish. Afterwards, concentrations stabilize between 4-23 pg/g in sediment, between 0.02-44 pg/L in water, and between 7-104 pg/g wet weight in fish, depending on compound and region. South Bay had the greatest final concentrations of pollutants, regardless of compartment. Fish consumption is safe for most scenarios, but due to model uncertainty, limitations in monthly intake could be established for North and South Bay catches.

Keywords

PFOA, PFOS, mass balance, San Francisco Bay, sediment, fish

1. Introduction

Perfluorooctanoic acid (PFOA) and perfluorooctanesulfonic acid (PFOS) are the most extensively used per- and polyfluoroalkyl substances (PFAS). These synthetic chemicals are characterized by presenting a hydrophobic, fluorine-rich carbon chain attached to a hydrophilic functional group (Clara et al., 2008). Due to this amphiphilic behavior, these compounds have been widely used as surfactants and water and stain repellents in industrial, commercial and residential products, including nonstick coatings, textile treatments, and fire suppressing aqueous film-forming foams (AFFF) (US EPA, 2006). However, due to these same properties, PFOA and PFOS can interact with living cells and cause several impacts in human health such as liver damage, endocrine disruption, fertility decrease, and cancer (ATSDR, 2018; Kleszczyński and Składanowski, 2009). Because of this, these compounds are no longer manufactured in Europe and the United States from the early 2000s (Land et al., 2018). However, due to the stability of their C-F bonds, they are highly persistent in the environment, being still present in the environment of these regions (Blum et al., 2015; Bräunig et al., 2017).

Since PFOA and PFOS are highly stable, the development of predictive models that can forecast the fate and levels of these pollutants among different compartments (e.g. sediments, water,

atmosphere) of an environment is a need in order to evaluate possible risks to humans and biota. In this regard, rate constant models represent a simple and robust tool to achieve this goal (Mackay et al., 1994). In their approach, the environment is treated as a single box, where each compartment is considered as homogeneously mixed. Then, a set of differential mass balance equations (one per compartment) is set to estimate the variation of a mass of pollutant during a stablished time period (kg/d). These variation rates are calculated by multiplying the mass of pollutant in a given moment (kg) by a series of rate constants (i.e. not time depending) depicting the main processes of gains and losses of a pollutant in a given compartment for a designated time period (d^{-1}). Due to their simplicity and good performance, rate constant models have been applied to predict the long term concentrations and compartment distribution of different pollutants for entire aquatic ecosystems (Booty et al., 2005; Gobas et al., 2018; Xiao et al., 2008). However, this approach fails to provide spatial distribution of pollutants within the ecosystem, and more complex calculation efforts must be performed to obtain this information (Kaur et al., 2012).

As in other urban estuaries around the globe, a great arrange of pollutants has been recorded in San Francisco Bay (SFB)(SFEI, 2016). To forecast the distribution and concentrations of some of these pollutants in different compartments, several rate constant simulations have been applied for this estuary as a whole. Thus, it is possible to find studies focused on polychlorinated biphenyls (PCBs), polybrominated diphenyl ethers (PBDEs), methylmercury (MeHg), or polycyclic aromatic hydrocarbons (PAHs) in SFB (Davis, 2004; Greenfield and Davis, 2005; Oram et al., 2008; Yee et al., 2011). Concerning PFOA and PFOS, their presence has been reported in water, sediment, biota, wastewater, stormwater, and drinking water of SFB (Houtz et al., 2016; Houtz and Sedlak, 2012; Hurley et al., 2016; Sedlak et al., 2017; Sedlak and Greig, 2012). These pollutants follow a very distinct spatial distribution, experiencing significantly higher values in the south branch of the Bay than in the other regions (Sedlak et al., 2018). Therefore, the long-term modelling of PFOA and PFOS in SFB requires a sufficient spatial differentiation to appreciate geographical differences within the Bay and apply management measures accordingly.

The main objective of the present effort was to create a model able to predict the long-term fate and concentration of PFOA and PFOS in water, sediment, and fish of multi-embayment estuaries in order to apply future management actions and study possible consequences for human health. To accomplish that, a multi-box rate constant model incorporating time-varying external inputs was designed. The model was then applied to the case study of SFB to predict the concentrations of PFOA and PFOS in sediments and water of three different regions (i.e., North, Central, and South Bay). This model simulates the main processes involving the addition and removal of PFAS in these two compartments, and connects the three regions of SFB through water outflows and tidal exchanges. Finally, sediment and water predicted concentrations of PFOA and PFOS were used as inputs into a food chain model (Larson et al., 2018) to calculate levels of these compounds in a sport fish species consumed by local residents.

2. Material and methods

2.1. Model description

The model used in the present study was developed by Mackay et al. (1994) and adapted to the study of PFAS. In brief, our model treats the different spatial sections of an embayment (regions) as independent boxes comprising two homogeneously mixed compartments (water and sediments). These compartments experience time-dependent gains and losses of PFOA and PFOS. The sediments are assumed as part of the active sediment layer, which are able to exchange PFOA and PFOS with the water column and buried sediments. The water exchanges PFAS with sediments, adjacent bay regions/ocean and the atmosphere, and receives PFOA and PFOS from rivers, wastewater treatment plants, and rainwater. All these processes are synthetized in the following equations:

Equation 1: $$\frac{\Delta \boldsymbol{M_{Wi,j,k}}}{\Delta \boldsymbol{t}} = \boldsymbol{WI_{i,j,k}} + \boldsymbol{M_{Si,j,k}}(\boldsymbol{k_{SW1i,j}} + \boldsymbol{k_{SW2i,j}}) - \boldsymbol{M_{Wi,j,k}}(\boldsymbol{k_{Vi,j}} + \boldsymbol{k_{Oi}} + \boldsymbol{k_{WRj}} + \boldsymbol{k_{WS1i,j}} + \boldsymbol{k_{WS2i,j}})$$

Equation 2: $\frac{\Delta M_{S\,i,j,k}}{\Delta t} = M_{Wi,j,k}(k_{WS1i,j} + k_{WS2i,j}) - M_{Si,j,k}(k_{SW1i,j} + k_{SW2i,j} + k_{Bi,j} + k_{SRj})$

where $M_{Wi,j,k}$ and $M_{Si,j,k}$ are respectively the masses (kg) of PFAS in water and sediments expressed as function of region "*i*", compound "*j*", and moment "*k*". These variables are multiplied by different time-independent rate constants (k) expressed in days^{-1} (d^{-1}). These rates depict the exchange and transformation processes occurring within the bay, and are region and/or compound dependent.

Sediment resuspension rate is represented by $k_{SW1i,j}$. This parameter depicts the outflow of particle-bounded PFAS from sediments to water. This rate constant takes into consideration the two main processes of sediment outflow: transportation of small particles embedded in water and transportation of coarser particles by bed load transport forces (Wang and Andutta, 2013). The sedimentation rate ($k_{WS1i,j}$) represents the transfer of particle-bounded PFAS from water to sediments. This parameter correlates the fraction of PFAS in waterborne particles with their settling velocity provided in previous studies (MacLeod et al., 2005). Sediment-to-water diffusion rate is depicted as $k_{SW2i,j}$. This process portrays the losses of dissolved PFAS from sediment to water via diffusion. Opposite to this term is $k_{WS2i,j}$, the water-to-sediment diffusion rate. It represents the diffusion of water-dissolved PFAS from water to sediment. Volatilization rate is denoted by $k_{Vi,j}$, which represents the transfers of dissolved PFAS from water to air via vaporization. k_{WRj} and k_{SRj} represent respectively the degradation of both dissolved and particle-bounded PFAS in water and sediment respectively. These parameters are derived from their correspondent half-lives in water and sediment, and display the same value regardless of region treated. $k_{Bi,j}$ is the burial rate, representing the loses of PFAS from active sediment layer to buried sediment. It correlates the particle-bounded PFAS in sediments with their burial mass transfer coefficient. This coefficient was estimated from resuspension and sedimentation fluxes, since not specific values for this parameter are found in the literature (details in Supplementary Information). Finally, outflow rate is included as k_{Oi}. This parameter describes the losses of dissolved and particle-bounded PFAS in water via direct outflow and tidal exchange with adjacent

bay regions and the ocean. This variable is compound-independent, and it inverse number can be used as an estimation of water residence time.

Apart from the rate constants, we included in our approach a time dependent term. $WI_{i,j,k}$ represent the water inputs received in a region "*i*", for compound "*j*", in a given "*k*" moment, and it is expressed in the same units as $M_{Wi,j,k}$ and $M_{Si,j,k}$ (kg). This term includes the loads delivered by the rivers, sewage treatment plants effluents, stormwater run-off, direct precipitation (i.e. wet deposition), water outflows from up-water regions, and tidal exchanges with adjacent bay regions and the ocean. Since all the aforementioned processes were considered as time variable, $WI_{i,j,k}$ was calculated as a dynamic parameter. Mathematical developments to calculate the different addends of Equation **1** and Equation 2 are displayed in Supplementary Information.

To run the model, Equation **1** and Equation 2 were solved by means of an Excel spreadsheet in an time-stepping way using a one-day time step (i.e. Δt=1 d), as follows:

Equation 3: $$\boldsymbol{M_{Wi,j,k+1}} = \frac{\Delta \boldsymbol{M_{Wi,j,k}}}{\Delta \boldsymbol{t}} + \boldsymbol{M_{Wi,j,k}}$$

Equation 4: $$\boldsymbol{M_{Si,j,k+1}} = \frac{\Delta \boldsymbol{M_{Si,j,k}}}{\Delta \boldsymbol{t}} + \boldsymbol{M_{Si,j,k}},$$

where $M_{Wi,j,k+1}$ and $M_{Si,j,k+1}$ are respectively the masses of compound "*j*" in region "*i*" for a "*k+1*" day.

2.2. Sport fish exposure

Predicted concentrations in sediments and water obtained from the rate constant model described in Section 2.1 were used to calculate levels of PFOA and PFOS in fish tissue by using the model described in Larson et al. (2018). This model calculates the concentrations of PFAS in fish tissue based on its dietary pattern and water intake. Shiner surfperch (*Cymatogaster aggregata*) was selected as the model fish since it has a limited home range and has been used extensively as an indicator of localized organic contaminants (Gassel et al., 2011). Fish diet was modeled as follows: 60% of benthic invertebrates, 20% of plankton, 15% of pelagic invertebrates, and 5% of

sediment (Melwani et al., 2012). Concentrations of PFAS in benthic and pelagic invertebrates were calculated from sediment and water levels respectively, as described by Larson et al. (2018). Concentration in plankton were obtained from water concentrations as showed in Casal et al., (2017). All these inputs, along with sediment concentrations, were multiplied by a dietary biomagnification factor to obtain the dietary load of PFAS. Finally, this dietary contribution was added to the water intake to obtain the concentration of PFAS in fish tissue. A more detailed description of these calculations can be found in Supplementary Information.

2.3. Sensitivity and uncertainty analysis

To explore the effects of the different parameters in the model, a stepwise sensitivity analysis was performed. To this end, all the inputs used in the model were multiplied by 3 and 1/3, and response ratios were calculated according to Yee et al. (2011) :

Equation 5: $\%\ Response\ ratio = \frac{\Delta Output/Output_{base}}{\Delta Input/Input_{base}} \times 100$

Variables having an additive response ratio (i.e., sum of absolute response ratio values in every region and compartment) equal to or greater than 100% were considered as highly influential. These variables were subjected to Monte Carlo simulations to evaluate the uncertainty of the model. To achieve this, a set of iterative combinations of random numbers among the range of values of the highly influential parameters obtained from the sensitivity analysis were performed. Minimum and maximum values used to obtain ranges are showed in Tables S2-S4. If no range has been found in the literature for a given variable, a range of ± 25% of base case value is considered. Afterwards, 95% prediction bands were provided as graphical representation to depict uncertainty.

3. Case of study

3.1. Area of study

The model described in Section 2.1 was applied to the case of San Francisco Bay (SFB). SFB is the largest estuary on the west coast of the Americas, and it is surrounded by a population of seven

million people (Figure 1). Most of the freshwater that flows into SFB comes via the Sacramento-San Joaquin River Delta entering the northern portion of the Bay, while water exchange with the ocean occurs largely in the central part of the Bay through the Golden Gate Strait. The southern part of the Bay has a reduced freshwater supply, much of which is treated wastewater effluent, and acts as a quasi-isolated lagoon (Walters et al., 1985). Accordingly, to study the dynamics of PFAS in SFB, three separate regions were taken into consideration: North Bay (from Sacramento-San Joaquin River Delta to the segment joining Point San Pablo and Point San Pedro), Central Bay (delimited in the north by the North Bay, and in the south by the line from Hunters Point to Bay Farm Island), and South Bay (all water to the south of the Central Bay). Each region of the Bay was treated as an independent box, and a Equation **1** and Equation 2 were applied to each one of them.

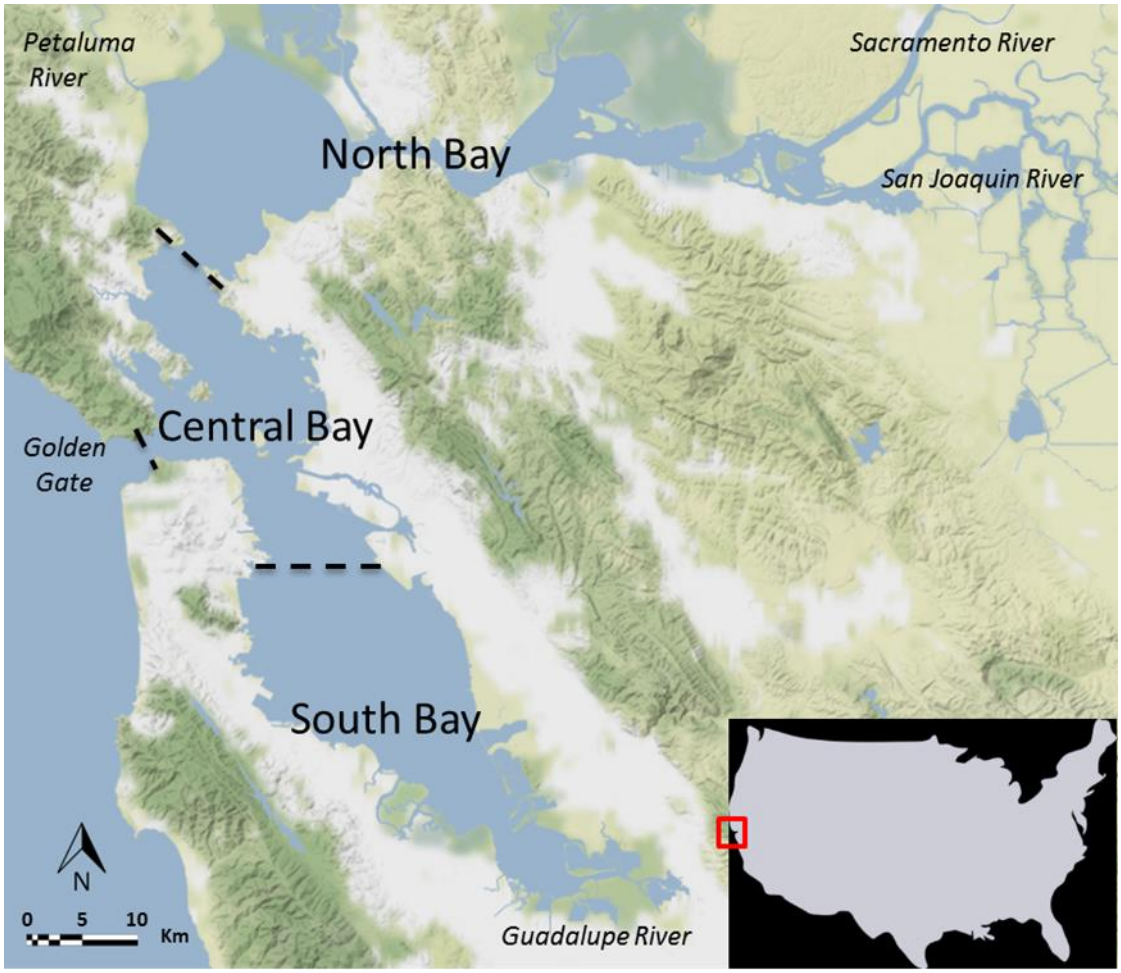

Figure 1: San Francisco Bay. Dashed lines represent the boundaries between the different regions of the Bay and the ocean. Source: Stamen Design.

3.2. Base case simulation

For the base case scenario, best estimated 2009 values for every parameter were used, as depicted in Tables S2 and S3. Region specific initial concentrations of PFAS in water and sediment were obtained as the average value of concentrations measured in different sampling points in 2009 ($C_{Wi,j,0}$ and $C_{Si,j,0}$; Table S2) (Sedlak et al., 2018). In cases where measured $C_{Wi,j,0}$ and $C_{Si,j,0}$ were below limits of detection, half the limit of detection was used. To obtain a more representative $C_{Wi,j,0}$, only mid-Bay (i.e., near-shore margins sites discarded) concentrations were used. Furthermore, to fulfill the same goal, initial concentrations in South Bay ($C_{Wsouth,j,0}$ and $C_{Ssouth,j,0}$), were calculated using weighting coefficients applied of 0.91 and 0.09 were applied respectively to Upper South Bay (i.e. north of Dumbarton Bridge) and Lower South Bay (i.e. south of Dumbarton Bridge) sampled concentrations. These coefficients were calculated as the relative volume of every sub-embayment to total South Bay volume (Smith and Hollibaugh, 2006). Since 2009 $C_{Si,j,0}$ in North and Central Bay were not reported, these values were calculated by linear interpolation from 2004 and 2010 values (Sedlak et al. ,2018).

4. Results and discussion

4.1. Model validation

As initial approach, the model was run using the 2009 values described in Tables S2-S5 as inputs (base case scenario). Simulated values for 2014 were compared with actual values measured in sediments and fish in 2014 (Sedlak et al., 2018) (Table 1). Unfortunately, we could not compare the results for water, since no actual measurements have been carried out after 2009.

PFOA simulated values for 2014 in sediments were higher than average measured values, but within their range. However, 2014 simulated PFOS concentrations in North and Central Bay were out of the range of 2014 sampled values. To improve the accuracy of the predictions, we started adjusting those variables that presented a higher influence in the predictions for sediments and a greater base-case value uncertainty. Thus, as will be explained in Section 4.4, half-life in sediment ($t_{1/2Sj}$) is the most sensitive parameter in the prediction of PFAS in sediments. Since no specific

values for this compound were found in the literature, we initially used a $t_{1/2Sj}$ value identical to PFAS half-life in water ($t_{1/2Wj}$). Furthermore, the predicted sediment concentrations are highly sensitive to initial sediment concentrations ($C_{Si,j,0}$) especially in the case of PFOS (see Section 4.4 for more details). These initial concentrations in sediments presented a high degree of uncertainty in North and Central Bay, since they were not measured in 2009, and linearly interpolated values from the period 2004-2010 were used instead (Sedlak et al., 2018). To improve the $t_{1/2Sj}$, we multiplied $t_{1/2Wj}$ by the $t_{1/2Sj}/t_{1/2Wj}$ ratio obtained from the degradation rates used by Kong et al. (2018). Thus, $t_{1/2SPFOA}$ was equal to $t_{1/2WPFOA}$ multiplied by 0.125, and $t_{1/2SPFOS}$ was calculated as $t_{1/2WPFOS}$ times 3.09. Afterwards, initial PFOA and PFOS concentrations in sediments in North and Central Bay were adjusted to equalize simulated and actual values. Therefore, $C_{SnorthPFOA0}$ and $C_{ScentralPFOA0}$ were respectively multiplied by 1.12 and 1.25 (obtaining respective values of 0.14 and 0.16 ng/g), and $C_{Snorth,PFOS,0}$ and $C_{Scentral,PFOS,0}$ were multiplied respectively by 0.42 and 1.44 (obtaining respective values of 0.25 and 0.30 ng/g).

Regarding fish concentrations, PFAS comparison was highly uncertain. On the one hand, comparison could only be done in Central and South Bay, since no 2014 PFAS concentrations are reported for North Bay. On the other hand, only two and one catches were analyzed in Central and South Bay respectively, which reduces the variability of samples. PFOA showed a good agreement between simulated and measured values (Table 1). All shiner surfperch measures reported by Sedlak et al. (2018) were below limits of detection, coinciding with the simulated concentrations. Even after performing the sediment corrections explained in the above paragraph, PFOS showed predicted concentrations for 2014 higher than those measured in 2014. Within the fish exposure model, the dietary biomagnification factor for PFOS ($BMF_{FishPFOS}$) is the most sensitive parameter (see Section 4.4 and Table S8 and S9 for more details). Although no specific values for shiner surfperch were found in the literature, results were improved after using a better estimated value of 0.081, as described by Brandsma et al., (2011).

Table 1: Comparison of simulated and measured values in sediments and fish (ng/g) in 2014

			Simulated		Measured*			Deviation
			Initial	Corrected	Mean	Min	Max	(%)**
PFOA	North	Sediment	0.11	0.09	0.09	<0.09	0.10	+6.36%
		Fish	0.20	0.18	-	-	-	-
	Central	Sediment	0.12	0.11	0.11	<0.09	0.16	+1.43%
		Fish	0.21	0.20	<0.50	<0.50	<0.50	<60.0%
	South	Sediment	0.21	0.16	0.15	0.05	0.23	+6.25%
		Fish	0.38	0.29	<0.50	-	-	-
PFOS	North	Sediment	0.55	0.25	0.25	<0.18	0.47	+0.80%
		Fish	10.4	1.71	-	-	-	-
	Central	Sediment	0.14	0.30	0.30	<0.20	0.61	-0.63%
		Fish	3.28	1.48	1.42	<0.99	1.85	+4.05%
	South	Sediment	0.83	0.88	1.06	0.49	3.40	-17.0%
		Fish	16.2	4.85	3.72	-	-	-

*From Sedlak et al. (2018);** Calculated from corrected simulated values and mean measured values. Results expressed as % of mean measured values

4.2. Base case rate constants

Using the values shown in Tables S2-S5, and the corrections carried out in section 4.1, we obtained the rate constants shown in Table 2. Regardless of compound and Bay region, the outflow rate (k_{Oi}) was the rate constant displaying the highest effect on PFAS concentrations. Therefore, PFAS was primarily removed from the Bay through water outflows (Fi) and tidal exchanges among Bay regions and the Ocean ($We_{i\text{-}central}$ and $Te_{central\text{-}sea}$). However, the latter phenomena had a greater impact on k_O calculations. Tidal exchanges accounted for 82, 89, and 95% of the k_O values for North, Central, and South Bay respectively, acting as the most influential processes in the movement of pollutants within and outside SFB (Connolly et al., 2005; Smith and Hollibaugh, 2006). This parameter displayed values one order of magnitude lower in South Bay, meaning respective retention times are one order of magnitude higher in this region (i.e. 39 days) than in North and Central Bay (around 8 days in both cases).

Diffusion and degradation processes were the second most influential parameters in the model, displaying similar values among different regions of the Bay in the rage of 10^{-4}-10^{-6} d^{-1}. Degradation in sediment (k_{SR}) was the principal sink of PFAS in this compartment. Although sediment degradation rates are likely very site-specific, the information to appropriately assign differing $t_{1/2sj}$ values is not currently available, so uniform values were applied to all sub-embayments within each simulation. Consequently, PFOA k_{SR} values were one order of magnitude greater than in the case of PFOS. Other processes showed greater variations for different parts of the Bay. Sedimentation and resuspension rates ($k_{WS1i,j}$ and $k_{SW1i,j}$ respectively) were one order of magnitude lower in the Central Bay. This is due to a deeper water column and a lower concentration of particles in water (Cpw) in this region as a result of its direct connection with the Ocean (Sedlak et al., 2018). The burial parameter had the least effect on the model. This process is only present in South Bay, since the North and Central regions are net erosional (BCDC, 2016).

Comparing the compounds, the sedimentation process was more significant for PFOS, while diffusion from sediment to water was more important for PFOA. As pointed out in previous simulation studies, this is due to the greater affinity of PFOS for sediment and the greater attraction of PFOA for water, which is explained by the one order of magnitude higher value of PFOS K_{OW} (Lindim et al., 2016). However, it is important to highlight here that due to their amphiphilic characteristics, it is difficult to measure K_{OW} for PFAS (Mueller and Yingling, 2017). Therefore, modelled predictive values were used (Arp et al., 2006). To have more realistic simulations, organic carbon normalized partition coefficients (K_{OC}) for different parts of SFB could be calculated in future studies (Ahrens et al., 2011). PFOS volatilization is slightly higher than PFOA volatilization. As seen in other studies comparing several compounds, this result is a direct consequence of the higher Henry's law constant of PFOA (Greenfield and Davis, 2005). Finally, degradation rate in sediments is one order of magnitude higher for PFOA than for PFOS, as a consequence of the adjustment made in sediment half-life values ($t_{1/2Sj}$) described in section 4.1.

Table 2: Base case rate constant values (d^{-1})

	Symbol	PFOA			PFOS		
		North	Central	South	North	Central	South
Sedimentation	k_{WS1}	4.81E-07	4.48E-08	5.89E-07	3.32E-06	3.78E-07	4.08E-06
Water-to-sediment diffusion	k_{WS2}	5.24E-05	2.63E-05	6.47E-05	4.06E-05	2.49E-05	5.02E-05
Volatilization	k_V	8.20E-08	3.32E-08	7.00E-08	1.59E-07	7.88E-08	1.36E-07
Outflow	k_O	1.23E-01	1.23E-01	2.56E-02	1.23E-01	1.23E-01	2.56E-02
Degradation water	k_{WR}	2.06E-05	2.06E-05	2.06E-05	4.63E-05	4.63E-05	4.63E-05
Resuspension	k_{SW1}	5.06E-08	9.54E-09	4.52E-08	5.18E-08	9.60E-09	4.62E-08
Sediment-to-water diffusion	k_{SW2}	4.45E-05	4.45E-05	4.27E-05	5.10E-06	5.10E-06	5.29E-06
Burial	k_B	0.00E+00	0.00E+00	5.11E-09	0.00E+00	0.00E+00	5.22E-09
Degradation sediment	k_{SR}	1.65E-04	1.65E-04	1.65E-04	1.50E-05	1.50E-05	1.50E-05

4.3. Base case simulations

Despite showing different trends, a decline in the concentrations of PFOA and PFOS was observed in the different regions of Bay regardless of region and compartment when using 2009 values in sediment and water as inputs (Figure 2). The decreasing curves for a given compound and compartment tend, in the long term, to reach equal values for the different regions assessed.

Regardless of region and compound, initial concentrations in water decreased till reaching nearly stable-state values (i.e., $\Delta M_{Wij}/\Delta t \geq -10^{-5}$) after approximately 50 years of simulations. By then, initial concentrations have been reduced by more than 96% for PFOA and 99% for PFOS. Afterwards, water concentrations continued to decrease slightly until reaching nearly stable values among the different compartments (Figure 3). However, decreasing trends among the different Bay regions were very different. Concentrations of PFOA and PFOS in South Bay decreased drastically in the first year, rapidly reaching concentrations around 1.50 ng/L for both compounds. Afterwards, the concentrations of these two pollutants decreased following a moderately exponential trend. This spin-up period has been described in previous papers, and it is due to the non-constrained initial conditions (Yee et al., 2011). In our case, these could be

indicative of an overestimation of initial concentrations of PFAS in South Bay ($C_{Wsouth,j,0}$) since, after discarding margin samples, only two samples were used to obtain initial concentrations (Sedlak et al., 2018). Furthermore, these two samples were taken in summer, when values of $C_{Wsouth,j,0}$ could be higher than mean annual concentrations, but within the same order of magnitude (Munoz et al., 2019; Sakurai et al., 2010). A similar phenomenon occurs in Central Bay during the first year. In the case of PFOS a drastic decrease is observed, while PFOA shows an initial increase to a maximum (0.60 ng/L) before decreasing gradually until stabilization. As in South Bay, this is indicative of a misestimation of initial concentrations due to the fact that only one sample was taken in summer, and its value was below the detection limit for both compounds. For North Bay, a slight adjustment is also observed during the first 40 days of simulation for both compounds, showing an exponential decrease trend afterwards. This exponential decay presented a steeper slope in South Bay since the PFAS output/input ratio was 1% higher than in the rest of regions.

For sediments, the time to obtain nearly stable values (i.e., $\Delta M_{Sij}/\Delta t \geq -10^{-5}$) varied highly depending on the compound. PFOA reached this scenario after approximately 50 years, while PFOS needed close to 500 years to reach nearly steady-state levels. This result is a consequence of the higher sediment half-life and sediment affinity (expressed as K_{OW}) of PFOS versus PFOA (Arp et al., 2006). Regardless of compound, a bigger decrease is observed in South Bay, since it is the only region with loss of PFAS due to sediment burial. Despite this, nearly stable concentrations in the South Bay region (7.40 and 22.7 pg/g for PFOA and PFOS respectively) were higher than those simulated for North and Central Bay (4-5 pg/g for PFOA and 6-8 pg/g for PFOS) (Figure 3). This outcome is directly related to the higher initial sediment concentrations of both PFAS in South Bay, which plays an important role in the performance of the model, as discussed in section 4.4.

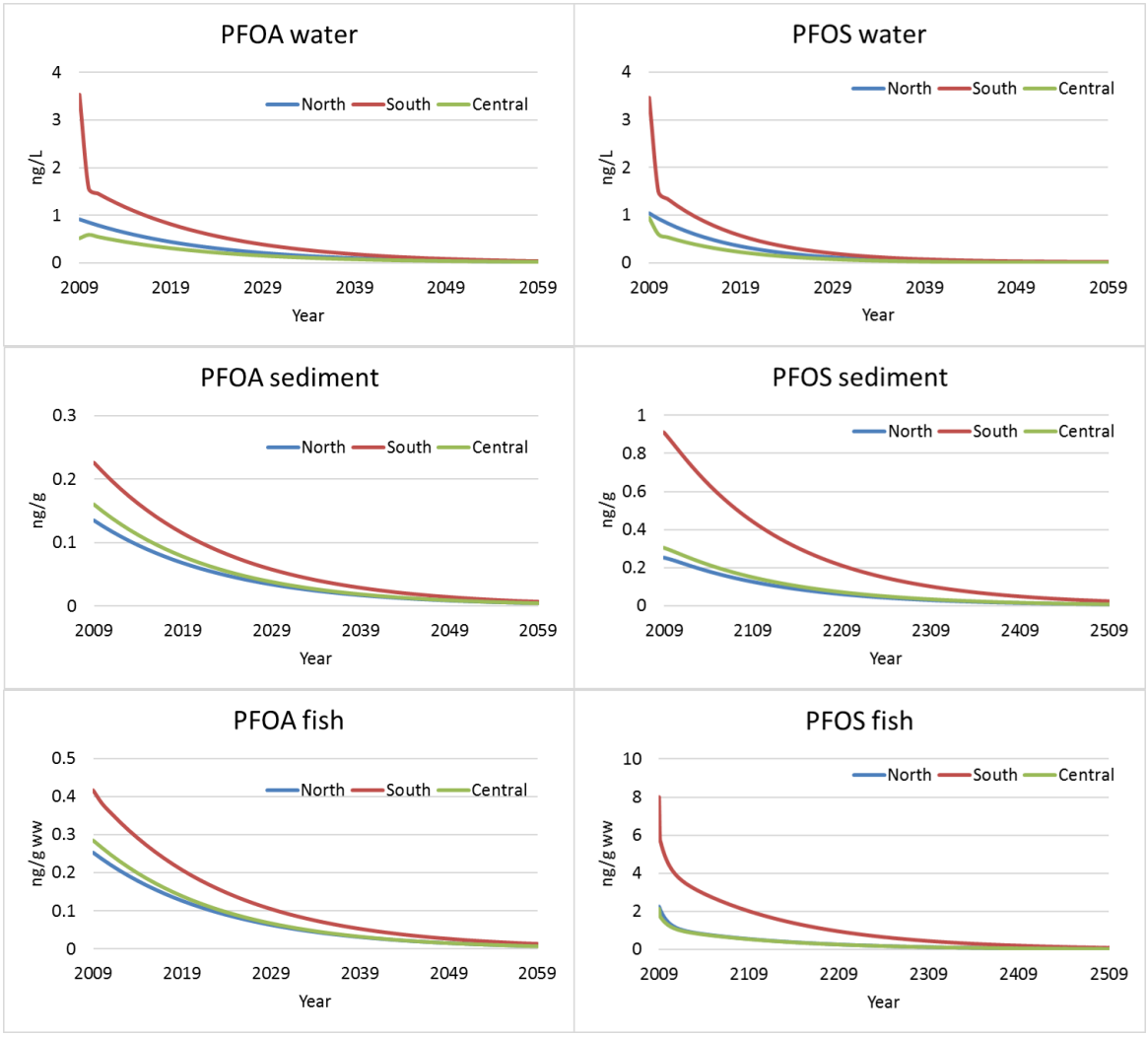

Figure 2: Base case simulations for PFOA and PFOS in water, sediment, and fish for different regions of the Bay.

Simulated values in fish reached their maximum values in South Bay in 2009. These values were around 0.4 and 8 ng/g of fish wet weight (ng/g ww) for PFOA and PFOS, respectively. These levels decreased subsequently till reaching nearly stable-state values between 7 - 14 pg/g ww in the case of PFOA and 29-104 pg/g ww for PFOS (Figure 3). However, decreasing trends depict different curves depending on the compound analyzed. PFOS simulations in fish show an initial trend parallel to water tendency, with sediment and water contributing equally to PFOS content in fish (i.e. 50.7 and 49.3% of PFOS fish concentrations are attributable to sediment and water respectively). These contributions are reduced to 98.2 and 1.7% for sediments and water respectively when reaching nearly stable-state values. In the case of PFOA, contributions to fish tissue are mostly attributed to sediments (more than 96% regardless of year). These differences

between PFOS and PFOA are a consequence of different values of fish exposure parameters, and more specifically, bioaccumulation from water-fish (BCF_{fish}), which is three orders of magnitude higher for PFOS than PFOA (Martin et al., 2003). Obtained results highlight the higher sensitivity of fish tissue for PFOS, which could be rapidly affected by peak concentrations in water. Therefore, special attention should be paid to PFOS when fish consumption is assessed after uncontrolled releases from products comprising this compound, such as older formulations of AFFF (Awad et al., 2011; Oakes et al., 2010). Regardless of year, simulated PFOS concentrations were lower than human dietary recommendations established by the State of Michigan (not more than 9 ng/g ww of PFOS in fish tissue consumed for sixteen meals per month) and the State of Minnesota Department of Public Health (no intake restriction for fish containing less than 10 ng/g ww of PFOS) (MDHHS, 2016; Minnesota Department of Health, 2019). However, in a preliminary report, the State of New Jersey presented more restrictive dietary recommendations for PFOS (i.e., 0.56, 3.9, and 17 ng/g ww for unlimited, weekly, and trimestral fish consumption respectively)(Goodrow et al., 2019). Despite these values should not be perceived as regulatory limits, they could act as indicators of potential harmful outcomes.

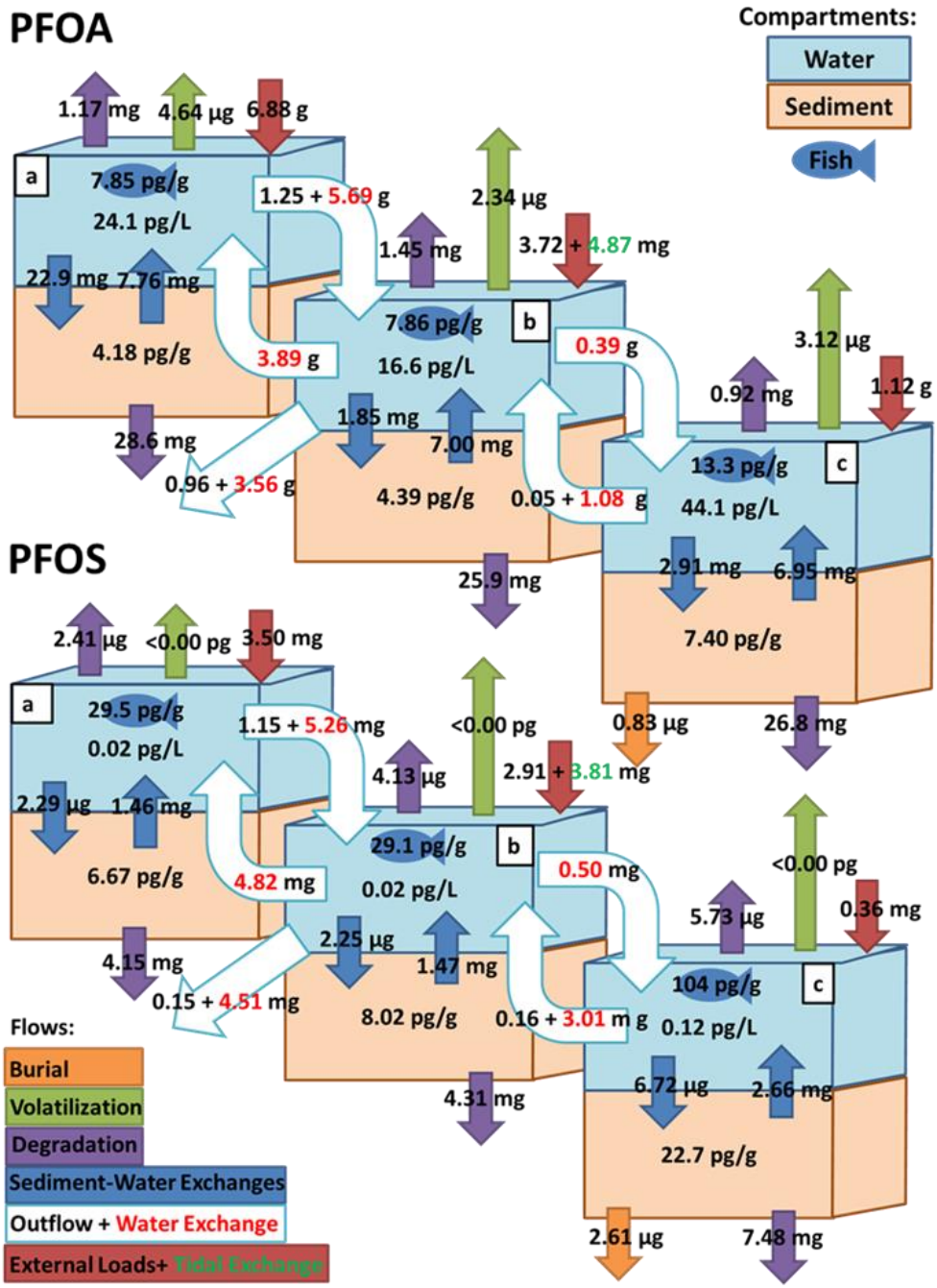

Figure 3: Steady-state scenario concentrations in water, sediment, and fish, and daily fluxes among the different parts of the Bay and the ocean after reaching nearly steady-state scenario for all compartments (i.e., 50 years for PFOA and 500 years for PFOS). a= North Bay; b= Central Bay; c=South Bay.

4.4. Sensitivity and uncertainty

Considering that nearly stable-state (i.e., daily variation of concentration in every compartment below 10^{-5}) are reached after 50 and 500 years for PFOA and PFOS, respectively, these time

lapses were chosen to study sensitivity of the model. Parameters showing a response ratio ≥ 1% for any compartment are reported in Tables S6-S9. Results differed depending on chemical compound, region, compartment, and variation applied to inputs (i.e., times three or one third). In case of multiplying inputs by three, the overall most influential parameter for PFOA and PFOS was sediment half-life ($t_{1/2Sj}$). Response ratios around 1700 % in sediment and fish were displayed when increasing $t_{1/2SPFOA}$ by three. However, this parameter had a minor influence in water (values lower than 15% regardless of region). Sediment half-life of PFOA ($t_{1/2SPFOA}$) is inversely related to degradation in sediment rate constant (k_{SRPFOA}), which, in the case of PFOA, is the second most influential rate constant (showing values in the range of 10^{-4}, see Table 2). Increasing $t_{1/2SPFOA}$ by three triggers a close to thirty-fold decrease in k_{SRPFOA} values, which in turn increases the levels of PFOA in sediments. For PFOS, increasing $t_{1/2SPFOS}$ by three increased base case values in sediment, fish, and water around 318% regardless of region. Sediment half-life of PFOS ($t_{1/2SPFOS}$) is more than ten times smaller than $t_{1/2SPFOA}$, and its correspondent k_{SRPFOS} values are in the range of 10^{-5}. These values are smaller than other rate constant, which limit their influence in sediment and fish. However, this parameter had a great influence in water, since it increases the sediment-to-water exchanges, which are the biggest source of PFOS in water (Figure 3). This phenomenon does not have the same importance for PFOA, since the biggest source of this compound in the Bay as a whole are the external loads.

Apart from $t_{1/2Sij}$, external loads (L_{iPFOA}), octanol-water constant (k_{OWPFOA}), initial concentration in sediments ($C_{Si,PFOA,0}$), and biota-sediment accumulation factor ($BSAF_{BIj}$) influence highly the outcomes of the model in terms of PFOA. These parameters are characterized by having a great influence in one or two compartments, while causing no or small variances in others. Thus, $BSAF_{BI\ PFOA}$ only affected concentration in fish, L_{iPFOA} had a greater impact in water (response ratios higher than 90% in every region) than in sediments and fish (23% maximum response ratio), and $M_{S0iPFOA}$ showed the opposite trend. Regarding PFOS, the most influential parameters were related to sediments, such as initial concentration in sediments ($C_{Si,PFOS,0}$), sediment depth (S_{depth}), concentration of solids in sediments (C_{SSi}) and density of sedimented solids (Dss) as the most

influential parameters. However, as explained in the case of $t_{1/2SPFOS}$, these parameters displayed homogeneous response ratios in every compartment. Regardless of region and compound, organic carbon of sediment solids (OC_{SSi}) showed a unique behavior. When this parameter was multiplied by three, sediments showed increases in their associated response ratios, while the opposite trend is depicted for waters and fish. This result could be contradictory, since as seen in section 4.3, long term fish concentrations are strongly linked to sediment concentrations. However, as depicted in supplementary equation S32, concentration of PFOA and PFOS in benthic invertebrates (C_{BIiJ}) is directly correlated to the organic carbon normalized concentration of PFOS in sediment (C_{Sij}/OC_{SSi}). Despite the fact that increasing OC_{SSi} will trigger an increase in $C_{Si,j}$, this increase will be smaller than the corresponding threefold increase of OC_{SSi}. Consequently, the organic fraction of sediments, from which benthic invertebrates feed, will present a lower PFAS concentration (Higgins et al., 2007).

When reducing the inputs to one third of the initial values, the list of parameters showing additive response ratios greater than 100% increased. For PFOA, density of sediment solids (d_{ss}) was the parameter displaying the biggest response ratios for sediments (190-226%) and fish (187-224%). A 1/3 reduction of this parameter decreases diffusion from sediments to water to close to one third, resulting in the increase of sediment and fish concentration of PFOA. In the case of water, water outflow for the different regions of the bay ($F_{i,PFOA}$) was the parameter influencing the most. When reducing this parameter to 1/3 of its value, response ratios among the different parts of SFB were inversely related to their respective F/V_W ratios. Consequently, different values were obtained for North (205%), Central (286%), and South Bay (111%) waters. Sediment half-life ($t_{1/2SPFOA}$), water to sediment mass transfer diffusion coefficient (V_d), and octanol-water partition coefficient (K_{OWPFOA}) were, in decreasing order, the remaining top five most sensitive parameters for PFOA. Regarding PFOS, $t_{1/2SPFOS}$ was the parameter showing the greatest additive influence, followed in decreasing order by sediment depth (S_{depth}), concentrations of solids in sediment (Cssi), octanol-water partition coefficient (K_{OWPFOA}), and d_{ss}. As in the case of multiplying

parameters by three, PFOA displayed variable response ratios among compartments, while PFOS showed more homogeneous inter-compartment response ratios.

Regarding the uncertainty, a Monte Carlo analysis comprising more than 3000 simulations was performed. This number of simulations was established after applying the formulas displayed in Byrne (2013). The 95% uncertainty bands for water, sediments, and fish after performing the simulations are shown in Figure 4 and

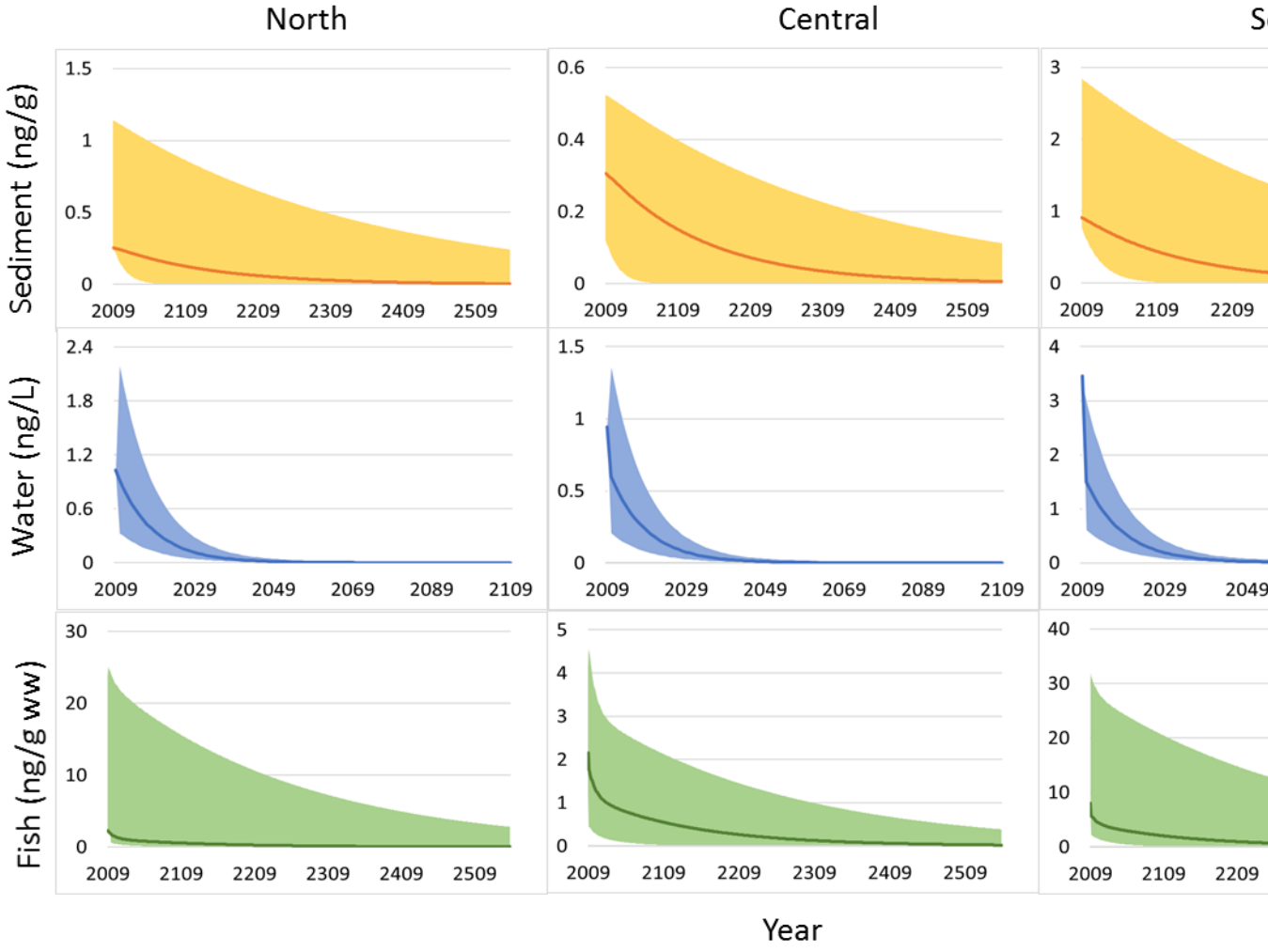

Figure 5. Uncertainty bands depicted nearly parallel curves to their correspondent base case curves till converging with them at nearly-stable state. For water, this scenario was reached at the same time as the base case scenario (i.e., after 50 years of simulation), while sediments and fish needed a time increase of 60% to get to this point (80 years for PFOA and 800 years for PFOS). Therefore, as base case simulations, uncertainty bands depict decreasing trends. The only parameter that could change this outcome would be time-dependent incremental or stable external loads. However, future temporal trends of external loads are likely to decline in line with the

phasing out of PFOA and PFOS (Wang et al., 2014). In fact, decaying trends during the last years have been reported in SFB effluents, as well as in other areas where PFAS regulations have been set up (Houtz et al., 2016; Land et al., 2018; Remucal, 2019; Sakurai et al., 2016). According to the characteristics of each compound, average width of uncertainty bands in water is higher for PFOA, while average width in sediments and fish is higher for PFOS. This fact has an important effect regarding fish consumption in North and South Bay. Unlike the base case predictions depicted in section 4.3, the upper uncertainty bands in these regions predicted restrictions in the fish intake. Thus, upper uncertainty band presented values within the range of 4 meals per month recommended by the State of Michigan (19-38 ng PFOS/g ww) for 49 years in North Bay and 123 years in South Bay (MDHHS, 2016). After 244 and 355 years for North and South Bay respectively, the upper uncertainty values descended till reaching the less restrictive dietary threshold (9 ng PFOS/g ww). Consequently, levels of PFOS in fish should be monitored in this period to ensure safe fish consumption recommendations.

Despite showing decaying trends, it is important to remark that the width of uncertainty bands and their associated time scale to reach nearly-stable concentrations in sediment and fish could change given the fact that the most sensitive model parameter ($t_{1/2Sj}$) in this exercise was estimated (see section 4.1). As some authors have recognized, this parameter is highly influenced by sediment composition (Ferrey et al., 2012; Venkatesan and Halden, 2014). Therefore, SFB specific values of $t_{1/2Sj}$ should be obtained to reduce the uncertainty of the predictions.

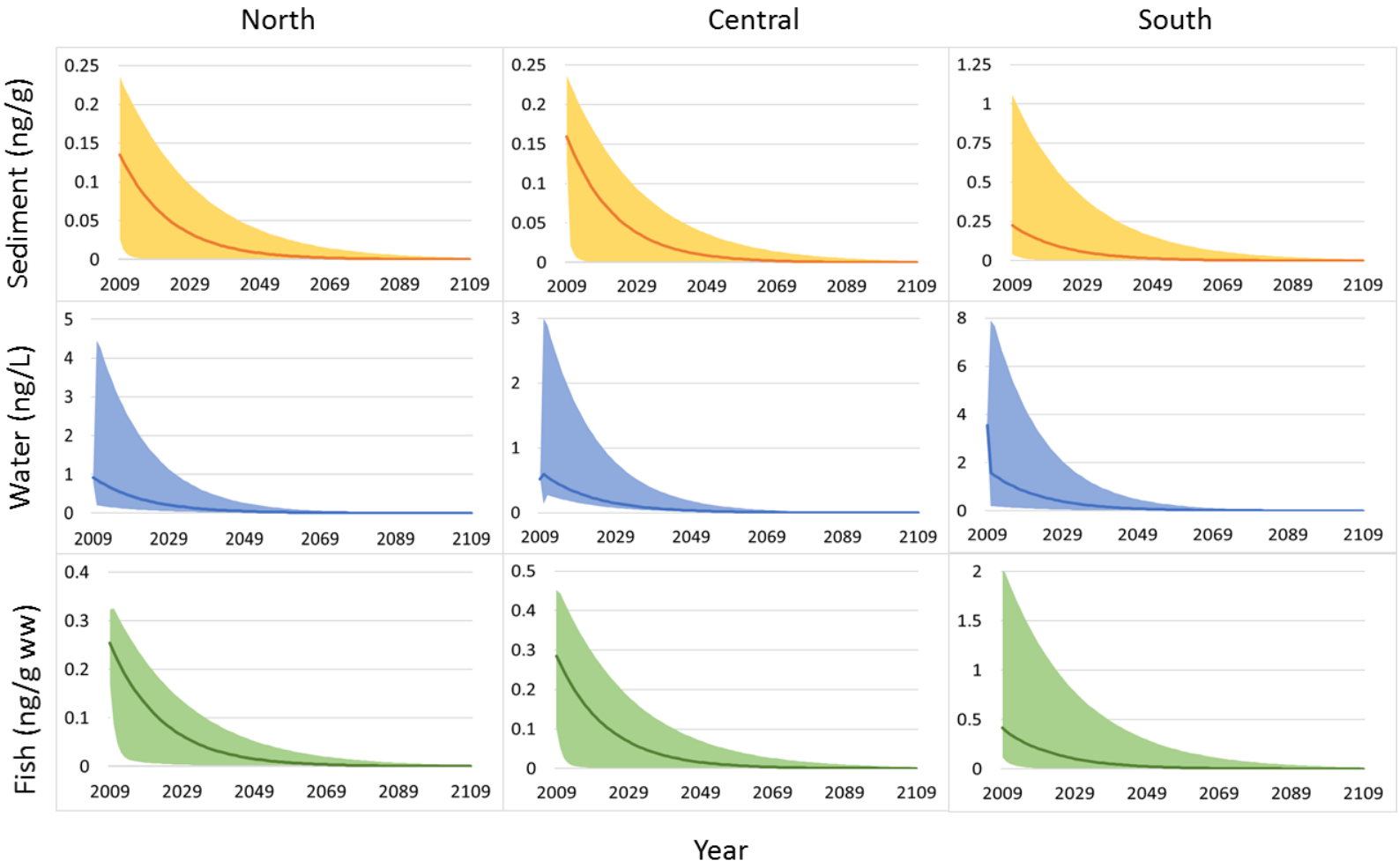

Figure 4: PFOA base case (bold) and uncertainty band (shaded) simulations for the different regions and compartments.

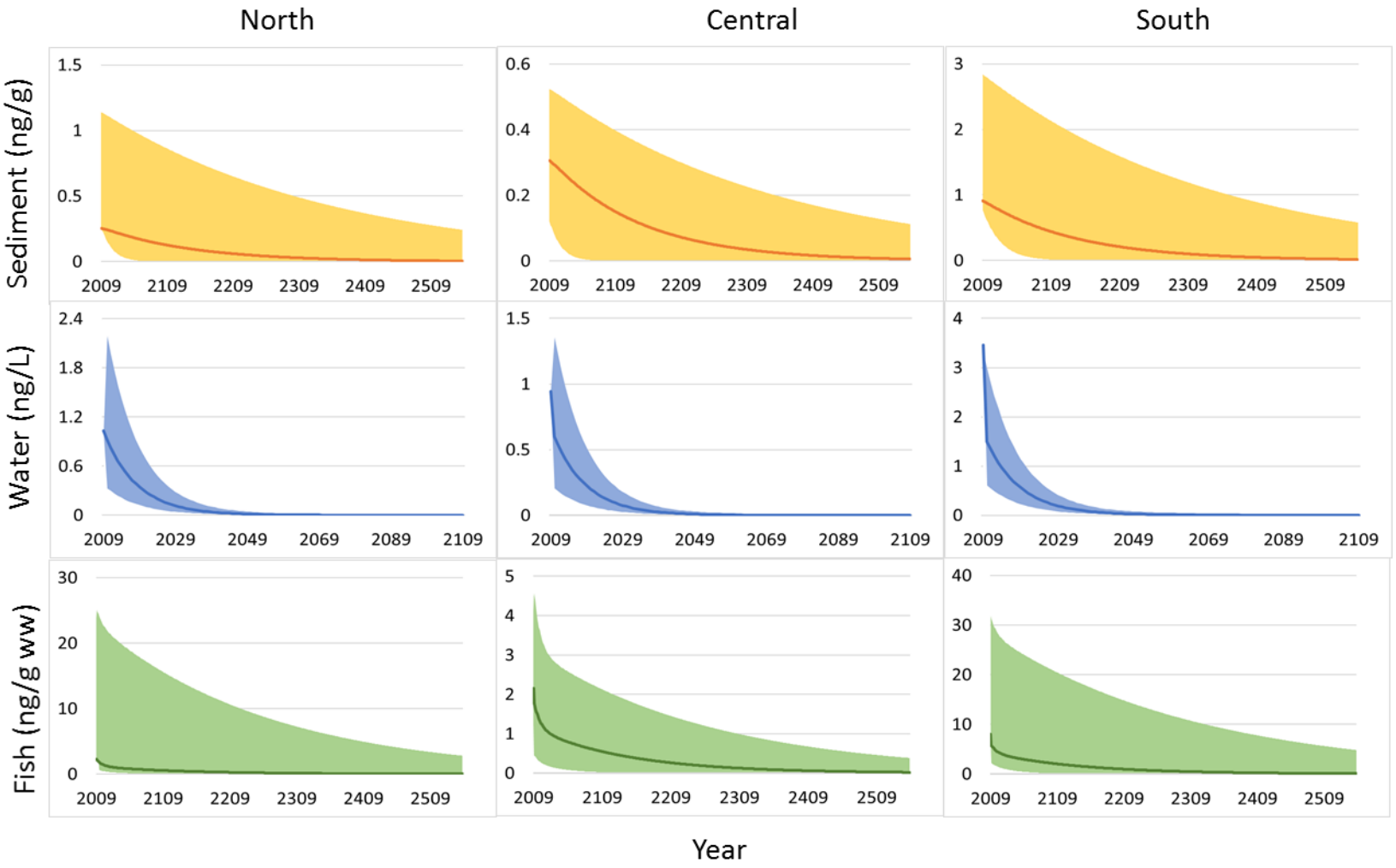

Figure 5 : PFOS base case (bold) and uncertainty band (shaded) simulations for the different regions and compartment

5. Conclusions and recommendations

In this paper, a multi-box rate constant model to forecast the fate and concentration of PFAS in estuaries comprising differential sub-embayments was developed. In order to study its performance, the model was tested in San Francisco Bay (SFB), which was divided into three regions (North, Central, and South). To better understand the potential risks to humans from the consumption of fish, our model was linked to a model that calculated PFAS concentrations in fish tissue (Larson et al., 2018). Our base case simulations (i.e., using 2009 monitoring data as inputs) showed an overall reduction in the content of PFOA and PFOS, in line with the decreasing trend in external sources of these compounds expected as a consequence of their phased out. Decreasing trends of PFAS were compound, compartment, and region dependent, influenced by the chemical properties of PFOA and PFOS, and the physical properties of the different compartments of the Bay. Thus, while PFOA declined to nearly stable concentrations after 50 years of simulation, PFOS levels in sediments and fish needed close to 500 years due to its higher sediment half-life ($t_{S1/2j}$). This parameter played a major role in the sensitivity of the model, which explains the higher levels and associated uncertainty in sediments and fish of PFOS. Fish consumption of a common sport fish species is predicted to be generally safe according to available tissue consumption guidance, but to comply with the inherent uncertainty of the model, limitations in monthly intake could be addressed if the catch is produced in North or South Bay.

The model here presented has proven useful to study the spatiotemporal distribution of PFAS in SFB, but has a number of limitations that should be addressed in the future. The base-case simulations obtained in this study present an inherent uncertainty resulting from a lack of input data for water, wastewater, stormwater, sediment, and precipitation. To overcome this limitation, we recommend that additional sampling be conducted. Furthermore, we were only able to compare simulated results in sediments, since no recent concentrations of PFAS in water were available. Regarding the chemical properties of PFAS, it is noteworthy that no SFB-specific values of $t_{S1/2j}$ are available. The values used were based on modeled calculations and are subject

to variability depending on the source consulted. Concerning PFAS fish exposure and human risks, some efforts should be developed in SFB to calculate fish ingestion rate for specific species, water bodies, and take into account PFAS content in fish tissue, as done by some environmental and health agencies (McKellar and Johnson, 2018; NJDEP and NJDOH, 2018). Finally, it is also important to consider the contributions of related compounds that degrade to PFOA and PFOS in the environment, known as precursors. Despite a lack of knowledge regarding some of their properties and toxicity, precursors are already found in the Bay and their impact should be evaluated (Sedlak et al., 2018).

Acknowledgements

The authors want to thank the E. U. Commission for the funding provided to the present study through the INTERWASTE project (EU H2020 734522). We are very grateful to Myrto Petreas for her job as coordinator of the aforementioned project. Additional support was provided by the Regional Monitoring Program for Water Quality in San Francisco Bay (RMP). Helpful comments were provided by J. Davis, A. Gilbreath and M. Diamond. The views expressed are those of the authors and do not necessarily reflect the views of the State of California.

Bibliography

Ahrens, L., Yeung, L.W.Y., Taniyasu, S., Lam, P.K.S., Yamashita, N., 2011. Partitioning of perfluorooctanoate (PFOA), perfluorooctane sulfonate (PFOS) and perfluorooctane sulfonamide (PFOSA) between water and sediment. Chemosphere 85, 731–737. doi:10.1016/j.chemosphere.2011.06.046

Arp, H.P.H., Niederer, C., Goss, K.U., 2006. Predicting the partitioning behavior of various highly fluorinated compounds. Environ. Sci. Technol. 40, 7298–7304.

doi:10.1021/es060744y

ATSDR, 2018. Toxicological profile for perfluoroalkyls. Draft for public comment. Agency for Toxic Substances and Disease Registry, Atlanta, GA.

Awad, E., Zhang, X., Bhavsar, S.P., Petro, S., Crozier, P.W., Reiner, E.J., Fletcher, R., Tittlemier, S.A., Braekevelt, E., 2011. Long-term environmental fate of perfluorinated compounds after accidental release at Toronto airport. Environ. Sci. Technol. 45, 8081–8089. doi:10.1021/es2001985

BCDC, 2016. Central San Francisco Bay regional sediment management plan. San Francisco Bay Conservation and Development Commission, San Francisco, CA.

Blum, A., Balan, S.A., Scheringer, M., Trier, X., Goldenman, G., Cousins, I.T., Diamond, M., Fletcher, T., Higgins, C., Lindeman, A.E., Peaslee, G., Voogt, P. De, Wang, Z., Weber, R., 2015. The Madrid statement on poly- and perfluoroalkyl substances (PFASs). Environ. Health Perspect. 123, A107--A111. doi:10.1289/ehp.1509934

Booty, W.G., Resler, O., McCrimmon, C., 2005. Mass balance modelling of priority toxic chemicals within the great lakes toxic chemical decision support system: RateCon model results for Lake Ontario and Lake Erie. Environ. Model. Softw. 20, 671–688. doi:10.1016/j.envsoft.2004.03.013

Brandsma, S.H., Smithwick, M., Solomon, K., Small, J., de Boer, J., Muir, D.C.G., 2011. Dietary exposure of rainbow trout to 8:2 and 10:2 fluorotelomer alcohols and perfluorooctanesulfonamide: Uptake, transformation and elimination. Chemosphere 82, 253–258. doi:10.1016/j.chemosphere.2010.09.050

Bräunig, J., Baduel, C., Heffernan, A., Rotander, A., Donaldson, E., Mueller, J.F., 2017. Fate and redistribution of perfluoroalkyl acids through AFFF-impacted groundwater. Sci. Total Environ. 596–597, 360–368. doi:10.1016/j.scitotenv.2017.04.095

Byrne, M.D., 2013. How many times should a stochastic model be run? An approach based on

confidence intervals. Proc. 12th Int. Conf. Cogn. Model. 445–450.

Casal, P., González-Gaya, B., Zhang, Y., Reardon, A.J.F., Martin, J.W., Jiménez, B., Dachs, J., 2017. Accumulation of perfluoroalkylated substances in oceanic plankton. Environ. Sci. Technol. 51, 2766–2775. doi:10.1021/acs.est.6b05821

Clara, M., Scharf, S., Weiss, S., Gans, O., Scheffknecht, C., 2008. Emissions of perfluorinated alkylated substances (PFAS) from point sources—identification of relevant branches. Water Sci. Technol. 58, 59–66. doi:10.2166/wst.2008.641

Connolly, J.P., Ziegler, C.K., Lamoureux, E.M., Benaman, J.A., Opdyke, D., 2005. Comment on "The long-term fate of polychlorinated biphenils in San Francisco Bay, (USA)." Environ. Toxicol. Chem. 24, 2397. doi:10.1897/04-537.1

Davis, J. a., 2004. The long-term fate of polychlorinated biphenyls in San Francisco Bay (USA). Environ. Toxicol. Chem. 23, 2396–2409. doi:10.1897/03-373

Ferrey, M.L., Wilson, J.T., Adair, C., Su, C., Fine, D.D., Liu, X., Washington, J.W., 2012. Behavior and fate of PFOA and PFOS in sandy aquifer sediment. Gr. Water Monit. Remediat. 32, 63–71. doi:10.1111/j.1745-6592.2012.01395.x

Gassel, M., Brodberg, R.K., Klasing, S. a., Cook, L.F., 2011. Health advisory and safe eating guidelines for San Francisco Bay fish and shellfish. California Office of Environmental Health Hazard Assessment, Sacramento, CA.

Gobas, F.A.P.C., Lai, H.-F., Mackay, D., Padilla, L.E., Goetz, A., Jackson, S.H., 2018. AGRO-2014: A time dependent model for assessing the fate and food-web bioaccumulation of organic pesticides in farm ponds: Model testing and performance analysis. Sci. Total Environ. 639, 1324–1333. doi:10.1016/j.scitotenv.2018.05.115

Goodrow, S.M., Ruppel, B., Lippincott, L., Post, G.B., 2019. Investigation of levels of perfluorinated compounds in New Jersey Fish, surface Water, and sediment. Contibution SR15-010. New Jersey Department of Environmental Protection Division of Science,

Research, and Environmental Health.

Greenfield, B.K., Davis, J.A., 2005. A PAH fate model for San Francisco Bay. Chemosphere 60, 515–530. doi:10.1016/j.compositesb.2014.04.020

Higgins, C.P., McLeod, P.B., MacManus-Spencer, L.A., Luthy, R.G., 2007. Bioaccumulation of perfluorochemicals in sediments by the aquatic oligochaete Lumbriculus variegatus. Environ. Sci. Technol. 41, 4600–4606. doi:10.1021/es062792o

Houtz, E.F., Sedlak, D.L., 2012. Oxidative Conversion as a Means of Detecting Precursors to Perfluoroalkyl Acids in Urban Runoff. Environ. Sci. Technol. 46, 9342–9349. doi:10.1021/es302274g

Houtz, E.F., Sutton, R., Park, J.S., Sedlak, M., 2016. Poly- and perfluoroalkyl substances in wastewater: Significance of unknown precursors, manufacturing shifts, and likely AFFF impacts. Water Res. 95, 142–149. doi:10.1016/j.watres.2016.02.055

Hurley, S., Houtz, E., Goldberg, D., Wang, M., Park, J.-S., Nelson, D.O., Reynolds, P., Bernstein, L., Anton-Culver, H., Horn-Ross, P., Petreas, M., 2016. Preliminary Associations between the Detection of Perfluoroalkyl Acids (PFAAs) in Drinking Water and Serum Concentrations in a Sample of California Women. Environ. Sci. Technol. Lett. 3, 264–269. doi:10.1021/acs.estlett.6b00154

Kaur, J., DePinto, J. V., Atkinson, J.F., Verhamme, E., Young, T.C., 2012. Development of a spatially resolved linked hydrodynamic and exposure model (LOTOX2) for PCBs in Lake Ontario. J. Great Lakes Res. 38, 490–503. doi:10.1016/j.jglr.2012.06.011

Kleszczyński, K., Składanowski, A.C., 2009. Mechanism of cytotoxic action of perfluorinated acids.: I. Alteration in plasma membrane potential and intracellular pH level. Toxicol. Appl. Pharmacol. 234, 300–305. doi:10.1016/J.TAAP.2008.10.008

Kong, X., Liu, W., He, W., Xu, F., Koelmans, A.A., Mooij, W.M., 2018. Multimedia fate modeling of perfluorooctanoic acid (PFOA) and perfluorooctane sulphonate (PFOS) in the

shallow lake Chaohu, China. Environ. Pollut. 237, 339–347. doi:10.1016/j.envpol.2018.02.026

Land, M., de Wit, C.A., Bignert, A., Cousins, I.T., Herzke, D., Johansson, J.H., Martin, J.W., 2018. What is the effect of phasing out long-chain per- and polyfluoroalkyl substances on the concentrations of perfluoroalkyl acids and their precursors in the environment? A systematic review. Environ. Evid. 7, 4. doi:10.1186/s13750-017-0114-y

Larson, E.S., Conder, J.M., Arblaster, J.A., 2018. Modeling avian exposures to perfluoroalkyl substances in aquatic habitats impacted by historical aqueous film forming foam releases. Chemosphere 201, 335–341. doi:10.1016/j.chemosphere.2018.03.004

Lindim, C., van Gils, J., Cousins, I.T., 2016. A large-scale model for simulating the fate and transport of organic contaminants in river basins. Chemosphere 144, 803–810. doi:10.1016/j.chemosphere.2015.09.051

Mackay, D., Sang, S., Vlahos, P., Diamond, M., Gobas, F., Dolan, D., 1994. A rate constant model of chemical dynamics in a lake ecosystem: PCBs in Lake Ontario. J. Great Lakes Res. 20, 625–642. doi:10.1016/S0380-1330(94)71183-7

MacLeod, M., McKone, T.E., Mackay, D., 2005. Mass balance for mercury in the San Francisco Bay area. Environ. Sci. Technol. 39, 6721–6729. doi:10.1021/es050112w

Martin, J.W., Mabury, S.A., Solomon, K.R., Muir, D.C.G., 2003. Bioconcentration and tissue distribution of perfluorinated acids in rainbow trout (Oncorhynchus mykiss). Environ. Toxicol. Chem. 22, 196–204. doi:10.1002/etc.5620220126

McKellar, J.D., Johnson, G.K., 2018. PFAS Fish Advisory. Media Release June 28 2018. Genesee County Health Department, Flint, MI.

MDHHS, 2016. Michigan fish consumption advisory program: guidance document version 4.0. Michigan Department of Health and Human Services, Lansing, MI.

Melwani, A.R., Greenfield, B.K., Yee, D., Davis, J.A., 2012. Conceptual foundations for modeling bioaccumulation in San Francisco Bay. RMP Technical Report 676. San Francisco Estuary Institute, Richmond, CA.

Minnesota Department of Health, 2019. Meal Advice Categories [WWW Document]. URL https://www.health.state.mn.us/communities/environment/fish/docs/eating/mealadvtbles.pdf (accessed 10.13.19).

Mueller, R., Yingling, V., 2017. History and use of per-and polyfluoroalkyl substances (PFAS). Fact sheet 11-13-2017. Interstate Technology Regulatory Council, Washington, DC.

Munoz, G., Budzinski, H., Babut, M., Lobry, J., Selleslagh, J., Tapie, N., Labadie, P., 2019. Temporal variations of perfluoroalkyl substances partitioning between surface water, suspended sediment, and biota in a macrotidal estuary. Chemosphere 233, 319–326. doi:10.1016/j.chemosphere.2019.05.281

NJDEP, NJDOH, 2018. Fish smart, eat smart: A guide to health advisories for eating fish and crabs caught in New Jersey waters. New Jersey Department of Environmental Protection and New Jersey Department of Health, Trenton, NJ.

Oakes, K.D., Benskin, J.P., Martin, J.W., Ings, J.S., Heinrichs, J.Y., Dixon, D.G., Servos, M.R., 2010. Biomonitoring of perfluorochemicals and toxicity to the downstream fish community of Etobicoke Creek following deployment of aqueous film-forming foam. Aquat. Toxicol. 98, 120–129. doi:10.1016/j.aquatox.2010.02.005

Oram, J.J., McKee, L.J., Werme, C.E., Connor, M.S., Oros, D.R., Grace, R., Rodigari, F., 2008. A mass budget of polybrominated diphenyl ethers in San Francisco Bay, CA. Environ. Int. 34, 1137–1147. doi:10.1016/j.envint.2008.04.006

Remucal, C.K., 2019. Spatial and temporal variability of perfluoroalkyl substances in the Laurentian Great Lakes. Environ. Sci. Process. Impacts 21, 1816–1834. doi:10.1039/C9EM00265K

Sakurai, T., Serizawa, S., Isobe, T., Kobayashi, J., Kodama, K., Kume, G., Lee, J.H., Maki, H., Imaizumi, Y., Suzuki, N., Horiguchi, T., Morita, M., Shiraishi, H., 2010. Spatial, phase, and temporal distributions of perfluorooctane sulfonate (PFOS) and perfluorooctanoate (PFOA) in Tokyo Bay, Japan. Environ. Sci. Technol. 44, 4110–4115. doi:10.1021/es1007609

Sakurai, T., Serizawa, S., Kobayashi, J., Kodama, K., Lee, J.-H., Maki, H., Zushi, Y., Sevilla-Nastor, J.B., Imaizumi, Y., Suzuki, N., Horiguchi, T., Shiraishi, H., 2016. Temporal trends for inflow of perfluorooctanesulfonate (PFOS) and perfluorooctanoate (PFOA) to Tokyo Bay, Japan, estimated by a receptor-oriented approach. Sci. Total Environ. 539, 277–285. doi:10.1016/j.scitotenv.2015.08.142

Sedlak, M., Sutton, R., Wong, A., Lin, D., 2018. Per and polyfluoroalkyl substances (PFASs) in San Francisco Bay : synthesis and strategy. SFEI Contribution No. 867. San Francisco Estuary Institute, Richmond, CA.

Sedlak, M.D., Benskin, J.P., Wong, A., Grace, R., Greig, D.J., 2017. Per- and polyfluoroalkyl substances (PFASs) in San Francisco Bay wildlife: Temporal trends, exposure pathways, and notable presence of precursor compounds. Chemosphere 185, 1217–1226. doi:10.1016/j.chemosphere.2017.04.096

Sedlak, M.D., Greig, D.J., 2012. Perfluoroalkyl compounds (PFCs) in wildlife from an urban estuary. J. Environ. Monit. 14, 146–154. doi:10.1039/C1EM10609K

SFEI, 2016. CD3 Tool. San Francisco Estuary Institute [WWW Document]. URL https://cd3.sfei.org/ (accessed 1.23.19).

Smith, S. V, Hollibaugh, J.T., 2006. Water, salt, and nutrient exchanges in San Francisco Bay. Limnol. Oceanogr. 51, 504–517.

Stamen Design, n.d. maps.stamen.com [WWW Document]. URL http://maps.stamen.com/#watercolor/12/37.7706/-122.3782 (accessed 11.29.18).

US EPA, 2006. Basic Information on PFAS- United States Environmental Protection Agency [WWW Document]. URL https://www.epa.gov/pfas/basic-information-pfas (accessed 11.27.18).

Venkatesan, A.K., Halden, R.U., 2014. Loss and in situ production of perfluoroalkyl chemicals in outdoor biosolids-soil mesocosms. Environ. Res. 132, 321–327. doi:10.1016/j.envres.2014.04.024

Walters, R.A., Cheng, R.T., Conomos, T.J., 1985. Time scales of circulation and mixing processes of San Francisco Bay waters. Hydrobiologia 129, 13–36. doi:10.1007/BF00048685

Wang, X.H., Andutta, P.F., 2013. Sediment Transport Dynamics in Ports, Estuaries and Other Coastal Environments, in: Sediment Transport Processes and Their Modelling Applications. InTech. doi:10.5772/51022

Wang, Z., Cousins, I.T., Scheringer, M., Buck, R.C., Hungerbühler, K., 2014. Global emission inventories for C4–C14 perfluoroalkyl carboxylic acid (PFCA) homologues from 1951 to 2030, Part I: production and emissions from quantifiable sources. Environ. Int. 70, 62–75. doi:10.1016/j.envint.2014.04.013

Xiao, Z., Yalan, Z., Shiyu, L., 2008. Ecological Risk Assessment of DDT Accumulation in Aquatic Organisms of Taihu Lake, China. Hum. Ecol. Risk Assess. An Int. J. 14, 819–834. doi:10.1080/10807030802235268

Yee, D., McKee, L.J., Oram, J.J., 2011. A regional mass balance of methylmercury in San Francisco Bay, California, USA. Environ. Toxicol. Chem. 30, 88–96. doi:10.1002/etc.366